

A Study on Synthesis and Exchange- Spring Properties of the SrFe₁₂O₁₉/Fe₃O₄ Nanocomposites with Core-Shell Structure

*Tran Thi Viet Nga**, *Luong Ngoc Anh*

Hanoi University of Science and Technology – No. 1, Dai Co Viet Str., Hai Ba Trung, Ha Noi, Viet Nam

Received: February 24, 2020; Accepted: June 22, 2020

Abstract

Two series of SrFe₁₂O₁₉/Fe₃O₄ nanocomposites were prepared using mechanical mixing method from SrFe₁₂O₁₉ and Fe₃O₄ nano powders and sol-gel method combined with hydrothermal method. The phase composition, surface morphology and magnetic properties of these samples were investigated using XRD, SEM, Raman and VSM. The stepped hysteresis loops of all the samples indicated that two magnetic phases are co-existed. Findings show that the samples prepared by using sol-gel method combine with hydrothermal method comprise two phases and Fe₃O₄ particles are coated on the surface of SrFe₁₂O₁₉ particles. The saturation magnetization reaches 63.735 emu/g for CS 950.

Keywords: nanocomposite, core- shell, exchange- spring.

1. Introduction

In recent years, as the magnetic nanomaterials have response ability for new applications technology and nano technology so the studies on magnetic nanoparticles combining the hard phase and the soft phase have become a hot research topic. According to Thomas Schrefl et al., in order to increase the saturation magnetization of the magnetically hard materials, we can insert the magnetically soft particles with higher saturation magnetization [1]. The exchange coupling between the two phases are enhanced, so it can significantly improve the physical properties of materials. Among the magnetically hard materials: Nd₂Fe₁₄B, SmCo₅... hexaferrite has been widely used due to its low cost and excellent oxidation corrosion resistance. So it is widely used in many applications, such as micro- magnet production, magnetic recording, GHz electronic components and electromagnetic absorbers (Radar Absorption Materials) using advanced composite materials mixed with carbon nanotubes, multiferroic materials... [2-4]. Nowadays, many researchers pay much attention to the researches of nanocomposite particles or core/shell structured nanoparticles basic on hexaferrite. Some results on hexaferrite particles can be mentioned as: BaM/Ni_{0.8}Zn_{0.2}Fe₂O₄ [5], BaFe₁₂O₁₉/CoFe₂O₄ [6], BaFe₁₂O₁₉/Fe₃O₄ [7],... It is well known that Fe₃O₄ is magnetically soft material with high saturation magnetization (94 emu/g). Hence, it could be a magnetically soft material for enhancing the magnetic properties of hexaferrite. Comparing the nanocomposite particles, contact area between the

aggregated particles in core/shell structure nanoparticles is extended so that they could be sufficiently exchange coupled. In the current work, we have used the mechanical mixing method from SrFe₁₂O₁₉ and Fe₃O₄ nano powders and sol-gel method combined with hydrothermal method to fabricate the SrFe₁₂O₁₉/Fe₃O₄ nanocomposites with core-shell structure. The phase composition, surface morphology, and magnetic properties of two series samples are investigated and compared.

2. Experiments

Synthesis of SrFe₁₂O₁₉ and Fe₃O₄ particles

In order to synthesis SrFe₁₂O₁₉ particles, we used the sol-gel method with the technical parameters, that is, the pH is 1, the molar ratio of (Sr²⁺+Fe³⁺)/C₃H₄(OH)(COOH)₃ is 1/3, the evaporated temperature is 80°C, the gel was dried at 100°C for 24h and then heated at 500°C for 2h. These technical parameters are obtained from our previous work. Finally, the gel was calcined in air at 850°C, 900°C, and 950°C for 2 hours.

The synthesis of the magnetically soft material, Fe₃O₄ nanoparticles was done by hydrothermal method. In a typical process, FeCl₂ and FeCl₃ were dissolved in deionized water with ratio of Fe²⁺: Fe³⁺ at 1: 2. NaOH 1M was then added into the solution at a fixed Fe²⁺: Fe³⁺ : NaOH molar ratio of 1: 2: 3. The solution was stirred at 1000 rpm in 15 minutes and transferred to an autoclave which was heat at 180°C for 12 hours. The black products were washed many times with deionized water and dried 60°C for 2 hours in vacuum.

* Corresponding author: Tel.: (+84) 983810608
Email: vietnga@itims.edu.vn

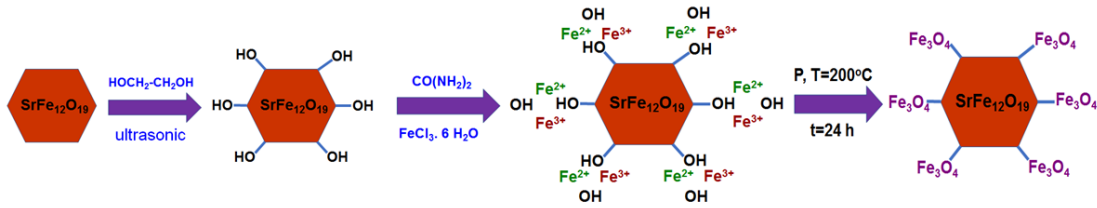


Fig. 1. Schematic procedure of the formation of the core-shell structure $\text{SrFe}_{12}\text{O}_{19}/\text{Fe}_3\text{O}_4$ nanocomposites

Synthesis of $\text{SrFe}_{12}\text{O}_{19}/\text{Fe}_3\text{O}_4$ nanocomposite particles using mechanical mixing method

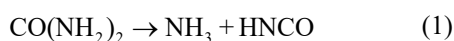
The first series of specimens of $\text{SrFe}_{12}\text{O}_{19}/\text{Fe}_3\text{O}_4$ nanocomposite powders were synthesized using the $\text{SrFe}_{12}\text{O}_{19}$ and Fe_3O_4 particles obtained previously. $\text{SrFe}_{12}\text{O}_{19}$ and Fe_3O_4 nanoparticles were mixed with mass ratios $\text{SrFe}_{12}\text{O}_{19}:\text{Fe}_3\text{O}_4$ of 1: 3. The samples of $\text{SrFe}_{12}\text{O}_{19}/\text{Fe}_3\text{O}_4$ with the $\text{SrFe}_{12}\text{O}_{19}$ gel calcined in air at 850°C , 900°C , and 950°C were labeled as Mix-850, Mix-900 and Mix-950. Then the mixtures were sintered at 40°C for 30 min.

Synthesis of $\text{SrFe}_{12}\text{O}_{19}/\text{Fe}_3\text{O}_4$ nanocomposite particles using sol-gel method combined with hydrothermal method

The second series of specimens, total of 0.2 g of $\text{SrFe}_{12}\text{O}_{19}$ particles was pretreated by dissolving in 50ml ethylene glycol $\text{C}_2\text{H}_6\text{O}_2$ ultrasonically for 2 h. This solution was stirred at 1000 rpm and 50°C . Then, 0.75g $\text{FeCl}_3\cdot 6\text{H}_2\text{O}$ and 2.7g urea $\text{CO}(\text{NH}_2)_2$ were added to the mixture and stirred for 30 min. Then, we transferred this mixture in a Teflon-lined stainless-steel autoclave with a 100 ml capacity at 200°C and stored for 24h in an oven. Subsequently, the autoclave was air cooled to room temperature. Finally, the precipitated products were washed with deionized water and then dried at 100°C for 24h in vacuum. The samples of $\text{SrFe}_{12}\text{O}_{19}/\text{Fe}_3\text{O}_4$ nanocomposites with different core-shell structures (varying calcination temperatures from 850°C to 950°C and calcination time of 2h) were labeled as CS-850, CS-900 and CS-950. Fig.1 schematically illustrates the procedure for the synthesis of $\text{SrFe}_{12}\text{O}_{19}/\text{Fe}_3\text{O}_4$ nanocomposites.

Formation mechanisms

At temperature above 80°C , urea decomposes into HNCO and NH_3 (Eq.(1)). Under hydrothermal conditions, CH_3CHO , as reductant, is produced via the deprotonation of ethylene glycol molecule (Eq. (2)). NH_3 and HNCO encounter with H_2O forming $\text{NH}_3\cdot\text{H}_2\text{O}$ which further ionizes in water, producing hydroxide ions (OH^-) (Eq.(3), (4)).



Organic species, like glycolates CH_3CHO , can reduce ferric ion Fe^{3+} into ferrous ion Fe^{2+} (Eq. (5)). Fe^{3+} , together with Fe^{2+} which reduced from Fe^{3+} by CH_3CHO , is co-precipitated (Eq.(6)).



Characterization

The crystal structure and phases of the obtained samples were identified via X-ray powder diffraction (XRD) using a Siemens D5000 diffractometer ($\text{CuK}\alpha$ radiation, $\lambda = 1.54056 \text{ \AA}$). The morphology and the particle size were observed via scanning electron microscopy (SEM, JEOL-JSM 7600F). The Raman spectra were obtained using Raman spectrometer in the $200\text{-}1000 \text{ cm}^{-1}$ range. The magnetic properties were measured using a vibrating sample magnetometer (VSM, Lakeshore 7410) with applied magnetic fields of up to 15 kOe.

3. Results and discussion

Fig.2 shows the XRD diffractions of the $\text{SrFe}_{12}\text{O}_{19}$, Fe_3O_4 , Mix samples and CS samples. Fig. 1a shows the crystalline structure of pure $\text{SrFe}_{12}\text{O}_{19}$ and Fe_3O_4 nanoparticles. All the observed peaks of sample are close to the characteristic peaks in the JCPDS cards of $\text{SrFe}_{12}\text{O}_{19}$ (No.33-1340) and Fe_3O_4 (No. 89-2355). For the Mix and CS samples, all these diffraction patterns clearly show the characteristic diffraction peaks for the $\text{SrFe}_{12}\text{O}_{19}$ (\bullet) and (\circ) Fe_3O_4 and no other impurity peak. For the Mix samples, the diffraction peaks of $\text{SrFe}_{12}\text{O}_{19}$ at 34.42° and 35.8° overlap with the plane (311) of Fe_3O_4 located at 35.5° . Rietveld refinement of the XRD patterns was conducted using the FullProf software in profile matching mode to determine the lattice parameters and phase content which are indicated in Table 1. Such observation was also perceived when $\text{SrFe}_{12}\text{O}_{19}/\text{CoFe}_2\text{O}_4$ nanocomposites with core-shell structure were synthesized [8].

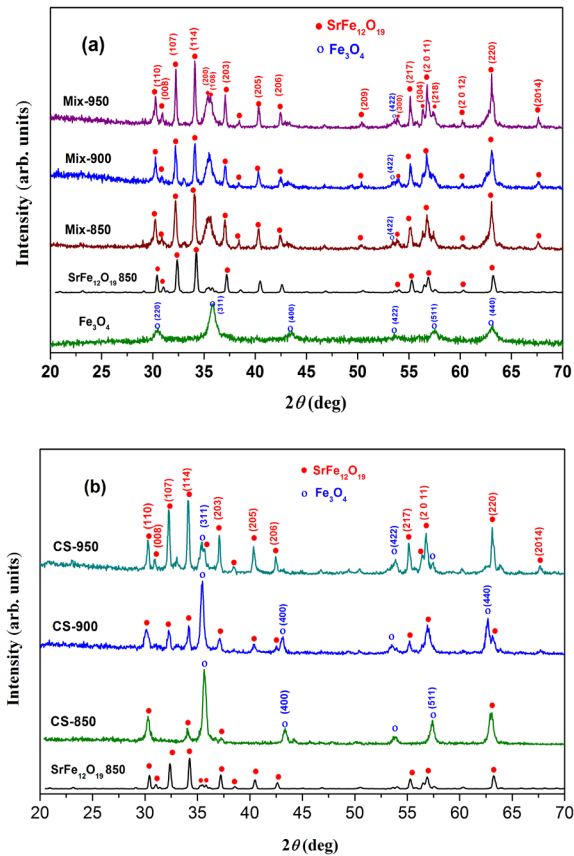


Fig. 2. XRD patterns of the nanocomposite powders: (a) $\text{SrFe}_{12}\text{O}_{19}$, Fe_3O_4 and $\text{SrFe}_{12}\text{O}_{19}/\text{Fe}_3\text{O}_4$ Mix-samples, (b) $\text{SrFe}_{12}\text{O}_{19}/\text{Fe}_3\text{O}_4$ CS- samples.

SEM images of Fe_3O_4 nanoparticles and Mix-850 nanocomposites are shown in Fig.3. The Fe_3O_4 nanoparticles have approximate diameter from 10 nm to 30 nm. The Mix-850 nanocomposite sample composed cubic grains (Fe_3O_4) with smaller size and hexagonal grains ($\text{SrFe}_{12}\text{O}_{19}$) with larger size, two phases are not well distributed. Thus, mechanical mixing method is an inadequate method for obtaining exchange-spring magnets because of non-homogenous distribution of magnetic phases.

Fig.4 shows the SEM images of the $\text{SrFe}_{12}\text{O}_{19}$ core and the $\text{SrFe}_{12}\text{O}_{19}/\text{Fe}_3\text{O}_4$ core-shell nanocomposites. All $\text{SrFe}_{12}\text{O}_{19}$ cores (Fig. 4a–c) exhibited a hexagonal platelet shape and a smooth

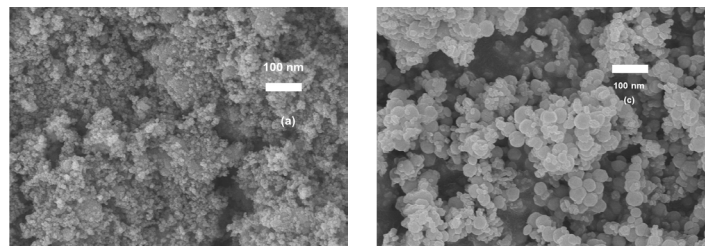


Fig. 3. SEM images of (a) Fe_3O_4 and (b) Mix- 850.

surface. The average particle size of these plate-like $\text{SrFe}_{12}\text{O}_{19}$ cores was evenly distributed in the range of 80–120 nm. The particles of CS-850, CS-900 and CS-950 displayed a spherical shape with a rough surface. The diameter of these particles was larger than those of the cores, respectively.

Table 1. XRD refinement results: lattice parameters (a, c) and percentages of phases present in the samples.

Sample	$\text{SrFe}_{12}\text{O}_{19}$			Fe_3O_4	
	a (Å)	c (Å)	%	a (Å)	%
$\text{SrFe}_{12}\text{O}_{19}$ 850	5.7827	23.037	~100		
Fe_3O_4				8.390	~100
Mix- 850	5.852	22.932	62.2	8.391	37.4
Mix- 900	5.852	22.932	62.2	8.388	37.4
Mix- 950	5.853	22.933	61.98	8.390	38.02
CS- 850	5.7827	23.679	31.28	8.346	66.41
CS- 900	5.871	23.021	39.91	8.367	55.84
CS- 950	5.834	23.771	72.95	8.348	23.02

It confirmed that Fe_3O_4 microspheres were deposited on the surface of $\text{SrFe}_{12}\text{O}_{19}$ particles. The obtained nanocomposites with core-shell structure are clearly spherical because of the increase in the calcination time of the core. These results agreed with

those reported by Ying Lin et. al [9]. The Raman spectra of the core $\text{SrFe}_{12}\text{O}_{19}$ (calcined at 850°C for 2h), Fe_3O_4 particle and CS-850 nanocomposites with core-shell structure were measured at room temperature to confirm the presence of $\text{SrFe}_{12}\text{O}_{19}$ and Fe_3O_4 phases in nanocomposites with core-shell structure. The results are shown in Fig.5. In the Raman spectrum, four modes of Fe_3O_4 291 cm^{-1} , 391 cm^{-1} , 490 cm^{-1} and 668 cm^{-1} can be seen in Fig.5a. And there are eight modes of $\text{SrFe}_{12}\text{O}_{19}$, namely, 225, 285, 335, 410, 468, 526, 613, and 680 cm^{-1} (Fig.5b). All modes of $\text{SrFe}_{12}\text{O}_{19}$ were found, and the 668 cm^{-1} mode of Fe_3O_4 was observed at CS-850 samples (Fig.4c). All modes have shifting tendency toward a low wave number. Combining Raman analysis, XRD and SEM results, we can conclude that core-shell structure of $\text{SrFe}_{12}\text{O}_{19}/\text{Fe}_3\text{O}_4$ nanocomposites have been successfully synthesized in CS-samples.

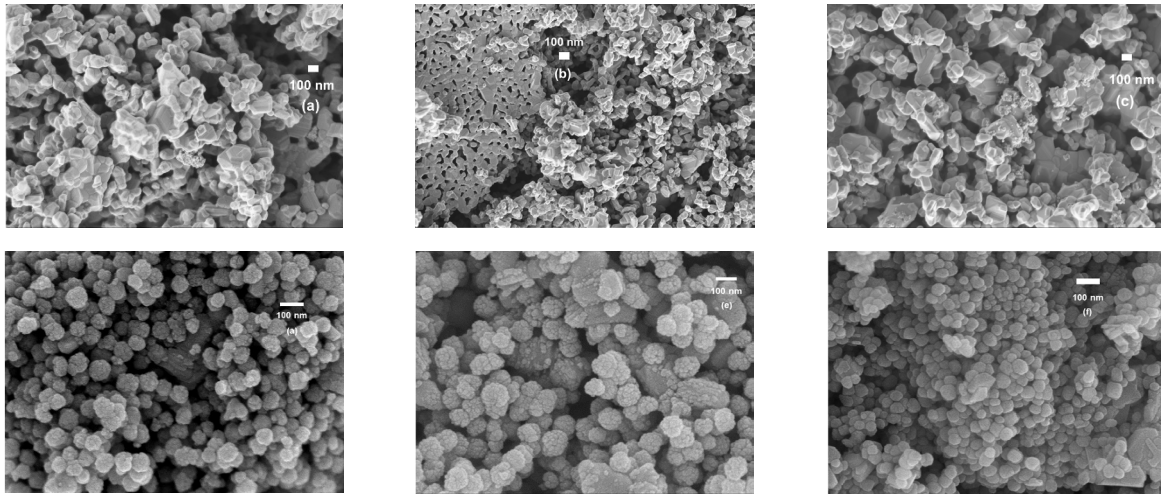


Fig. 4. SEM micrographs of SrFe₁₂O₁₉ core calcined at different temperature and SrFe₁₂O₁₉/Fe₃O₄ core-shell nanocomposite samples: (a) and (d) 850°C; (b) and (e) 900°C; (c) and (f) 950°C.

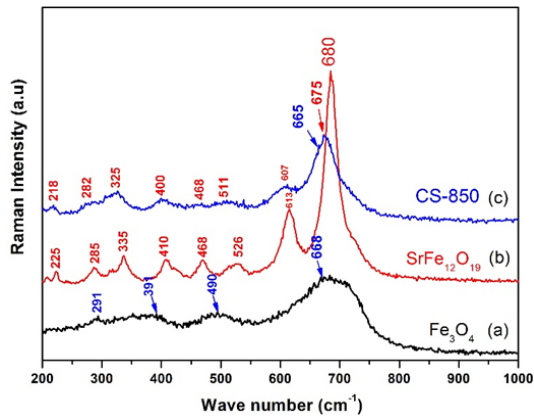


Fig. 5. Raman spectra of (a) Fe₃O₄ nanoparticles, (b) SrFe₁₂O₁₉ nanoparticles and (c) CS-850 nanocomposites.

The magnetic properties of the samples were measured at room temperature via VSM. The magnetization at 15 T (M), remanence magnetization (M_r) and coercivity (H_C) obtained from hysteresis loops are showed in Table 2. The Fig. 6 depicts the hysteresis loops of all samples at room.

The magnetization at 15 T (M), remanence magnetization (M_r) and coercivity (H_C) obtained from hysteresis loops are showed in Table 2. SrFe₁₂O₁₉ nanoparticles exhibit a magnetically hard behavior with the coercivity of 7 kOe and saturation magnetization of 60.30 emu/g. The hysteresis loop of Fe₃O₄ nanoparticles shows a magnetically soft behavior with the intrinsic coercivity of 0.59 kOe and saturation magnetization of 66.71 emu/g. While Mix-samples and CS-samples exhibited a typical bee waist. That is, they show the presence of two phases in the hysteresis loop instead of a single phase. It indicates the hard and soft magnetically phases are

switching individually due to the in-complete exchange-coupling.

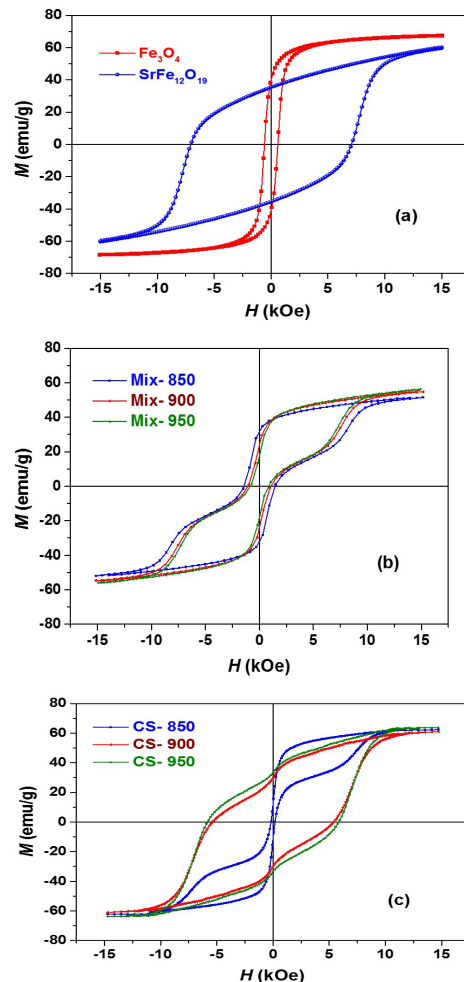


Fig. 6. Hysteresis loops of (a) the SrFe₁₂O₁₉ and Fe₃O₄, (b) Mix-samples and (c) CS-samples

For the Mix- samples, the coercivity decrease from 1.43 kOe to 0.88 kOe when the calcination temperature of core increased from 850°C to 950°C. It can be understood via the development of grain size and distribution size with increase in the calcination temperature. The coercivity H_C and saturation magnetization M_S of the CS-900 and 950 are larger than that of the Mix-900 and 950. For the composite particles, contact area between the aggregated particles is limited so that they could not be sufficiently exchange coupled. In the nanocomposite with the core-shell structure, the two phases contacted sufficiently, so magnetic properties of CS-samples can be improved. According to the SEM results (Fig.4), Fe_3O_4 microspheres were deposited on the surface of $SrFe_{12}O_{19}$ particles. The coercivity of all nanocomposite samples were smaller than those of $SrFe_{12}O_{19}$ core nanoparticles, probably due to the weak interaction between the two phases and the smaller H_C of the Fe_3O_4 core than the $SrFe_{12}O_{19}$ core.

For coercivity, exchange coupling occurred when the two phases made a contact with each other. In the magnetization process, the rotation of the domains in one particle induces domains in contiguous particles to rotate as the field is reversed, thereby decreasing coercivity [10]. The coercivity of CS-850 sample was the lowest. It may be due to the particle size of this core was the smallest. Hence, the Fe_3O_4 particles covered a thick layer on this core surface. The magnetic properties of this sample exhibited the magnetically soft phase of Fe_3O_4 (the coercivity was low, and the saturation was high). The coercivity H_C and saturation magnetization M_S of CS-950 reach 5.91 kOe and 63.73 emu/g.

4. Conclusion

In this paper, the $SrFe_{12}O_{19}/Fe_3O_4$ nanocomposites with core-shell structure is prepared successfully by combining sol-gel and hydrothermal methods. The Fe_3O_4 particles with a diameter smaller than 10 nm are coated on the surface of $SrFe_{12}O_{19}$, as shown in the SEM images. VSM results and XRD patterns confirmed the coexistence of two hard and soft phases. The coercivity and saturation magnetization of CS-samples are larger than that of Mix- samples. The homogeneity of phases, grain size, and exchange coupling between the two phases among others may result in variations in coercivity and saturation magnetization of the nanocomposite samples with core-shell structure.

Acknowledgment

The current work was financially supported by Hanoi University of Science and Technology (Grant No. T2018-PC-069).

References

- [1] T. Schrefl, H. F. Schmidts, J. Fidler, and H. Kronmüller, The role of exchange and dipolar coupling at grain boundaries in hard magnetic materials, *J. Magn. Magn. Mater.*, vol. 124, no. 3, pp. 251–261, 1993.
- [2] J. Buršík, Z. Šimš, L. Štichauer, and R. Tesař, Magneto-optical properties of Co- and Ti-substituted hexagonal ferrite films prepared by the sol-gel method, *J. Magn. Magn. Mater.*, vol. 157–158, pp. 311–312, 1996.
- [3] C. C. Yang, Y. J. Gung, C. C. Shih, W. C. Hung, and K. H. Wu, Synthesis, infrared and microwave absorbing properties of $(BaFe_{12}O_{19}/BaTiO_3)/polyaniline$ composite, *J. Magn. Magn. Mater.*, vol. 323, no. 7, pp. 933–938, 2011.
- [4] M. Chithra, C. N. Anumol, B. Sahu, and S. C. Sahoo, Exchange spring like magnetic behavior in cobalt ferrite nanoparticles, *J. Magn. Magn. Mater.*, vol. 401, pp. 1–8, 2016.
- [5] K. W. Moon, S. G. Cho, Y. H. Choa, K. H. Kim, and J. Kim, Synthesis and magnetic properties of nano Ba-hexaferrite/NiZn ferrite composites, *Phys. Status Solidi Appl. Mater. Sci.*, vol. 204, no. 12, pp. 4141–4144, 2007.
- [6] H. Yang, M. Liu, Y. Lin, and Y. Yang, Simultaneous enhancements of remanence and (BH)max in $BaFe_{12}O_{19}/CoFe_2O_4$ nanocomposite powders, *J. Alloys Compd.*, vol. 631, pp. 335–339, 2015.
- [7] K. P. Remya, D. Prabhu, S. Amirthapandian, C. Viswanathan, and N. Ponpandian, Exchange spring magnetic behavior in $BaFe_{12}O_{19}/Fe_3O_4$ nanocomposites, *J. Magn. Magn. Mater.*, vol. 406, pp. 233–238, 2016.
- [8] L. Zhang and Z. Li, Synthesis and characterization of $SrFe_{12}O_{19}/CoFe_2O_4$ nanocomposites with core-shell structure, *J. Alloys Compd.*, vol. 469, no. 1–2, pp. 422–426, 2009.
- [9] Y. Lin, Y. Liu, J. Dai, L. Wang, and H. Yang, Synthesis and microwave absorption properties of plate-like $BaFe_{12}O_{19}@Fe_3O_4$ core-shell composite, *J. Alloys Compd.*, vol. 739, pp. 202–210, 2018.
- [10] H. Zeng, S. Sun, J. Li, Z. L. Wang, and J. P. Liu, Tailoring magnetic properties of core/shell nanoparticles, *Appl. Phys. Lett.*, vol. 85, no. 5, pp. 792–794, 2004.